Retention of prominin in microvilli reveals distinct cholesterol-based lipid micro-domains in the apical plasma membrane

Katja Röper*†, Denis Corbeil*† and Wieland B. Huttner*‡

*Department of Neurobiology, Interdisciplinary Center of Neuroscience, University of Heidelberg, Im Neuenheimer Feld 364, D-69120 Heidelberg, and Max-Planck-Institute of Molecular Cell Biology and Genetics, Pfotenhauerstrasse 110, D-01307 Dresden, Germany
†These authors contributed equally to this work.
‡e-mail: whuttner@sun0.urz.uni-heidelberg.de

Membrane cholesterol–sphingolipid 'rafts', which are characterized by their insolubility in the non-ionic detergent Triton X-100 in the cold, have been implicated in the sorting of certain membrane proteins, such as placental alkaline phosphatase (PLAP), to the apical plasma membrane domain of epithelial cells. Here we show that prominin, an apically sorted pentaspan membrane protein, becomes associated in the *trans*-Golgi network with a lipid raft that is soluble in Triton X-100 but insoluble in another non-ionic detergent, Lubrol WX. At the cell surface, prominin remains insoluble in Lubrol WX and is selectively associated with microvilli, being largely segregated from the membrane subdomains containing PLAP. Cholesterol depletion results in the loss of prominin's microvillus-specific localization but does not lead to its complete intermixing with PLAP. We propose the coexistence within a membrane domain, such as the apical plasma membrane, of different cholesterol-based lipid rafts, which underlie the generation and maintenance of membrane subdomains.

As cells assemble to form tissues, the domain organization of the plasma membrane becomes increasingly complex. Paradigms include the epithelial cell and the neuron, the plasma membranes of which are divided into two major domains, the basolateral versus apical and the somatodendritic versus axonal, respectively[1,2]. Each domain is in turn composed of membrane subdomains. These can be very numerous, as exemplified by the dendritic arborization of a neuron, which receives hundreds to thousands of distinct synaptic inputs, or relatively few, as in the apical surface of an epithelial cell with its microvillar and non-microvillar subdomains[3].

The molecular interactions underlying the organization of the plasma membrane into domains and subdomains fall into two classes—'horizontal' interactions in the plane of the membrane between some of its constituents, and 'vertical' interactions between certain membrane constituents and the extracellular matrix as well as the subplasmalemmal cytoskeleton. Both of the two principal types of membrane constituent (proteins and lipids) can engage in either class of molecular interaction.

In the case of the apical plasma membrane domain of epithelial cells and its microvillar versus non-microvillar subdomains, two such interactions have been a focus of research. In the generation of the apical domain, a key role has been attributed to the horizontal interaction of certain membrane lipids (cholesterol and sphingolipids) with each other to form lipid 'rafts', which in turn interact with certain membrane proteins[4–6]. In the generation of the microvillar plasma-membrane subdomain, the vertical interaction of certain membrane proteins and lipids (phosphoinositides) with the underlying actin cytoskeleton is thought to be important.

In studying the molecular cell biology of neuroepithelial cells, which generate all neurons of the mammalian central nervous system, we previously identified the pentaspan plasma-membrane protein prominin[8]. The subcellular localization of prominin exhibits two notable features. First, in epithelial cells, prominin is sorted from the *trans*-Golgi network (TGN) to the apical plasma-membrane domain[9]. Second, in epithelial as well as non-epithelial cells, prominin is preferentially associated with a membrane subdomain (plasmalemmal protrusions). This is indicated by the specific localization of prominin in microvilli of the apical plasma membrane of epithelial cells, which occurs irrespective of the presence of tight junctions[8,9]; in the plasma-membrane evaginations at the base of the rod outer segment of retinal photoreceptor cells[10]; in plasma-membrane protrusions of haematopoietic stem cells[11]; and in microspikes and related plasma-membrane protrusions of transfected fibroblasts[8].

The molecular interactions underlying sorting of prominin to the apical plasma membrane domain and its preferential association with the protrusion-type plasma membrane subdomain are unknown. We have used polarized MDCK cells to investigate two questions. First, does the apical sorting of prominin involve its association with the lipid raft implicated in the apical sorting of other membrane proteins, and whose characteristic feature is insolubility in the non-ionic detergent Triton X-100 in the cold? Second, does the selective association of prominin with microvilli depend on its interaction with the subplasmalemmal actin-based cytoskeleton? Surprisingly, we find that neither is the case, and that both the apical sorting of prominin and its association with microvilli involve a novel cholesterol-based lipid raft.

Results

Cell-surface prominin is soluble in Triton X-100 but insoluble in Lubrol WX. We first investigated whether prominin is associated with the cholesterol–sphingolipid rafts that are recovered as detergent-insoluble complexes upon solubilization of cells in Triton X-100 at low temperature[12,13]. We used confluent prominin-transfected

Table 1 Comparison of the detergent-resistant complexes obtained with various detergents

Detergent	HLB	Chemical nomenclature	Prominin in pellet (%)	
			ER	PM
Triton X-100	13.5 (ref.48)	PEG (9-10)-octylphenyl ether	≤5	≤5
Triton X-102	14.6	PEG (12-13)-octylphenyl ether	8	66
Triton X-114	12.4 (ref.48)	PEG (7-8)-octylphenyl ether	≤5	11
Lubrol WX	14.9	PEG (17)-cetyl stearyl ether	≤5	43
Lubrol PX	–	PEG (9)-lauryl ether	≤5	≤5
Brij 56	12.9	PEG (10) cetyl ether	6	10
Brij 58	15.8 (ref. 49)	PEG (20) cetyl ether	11	60
Brij 35	16.9	PEG (23)-lauryl ether	75	91
Tween 20	16.7 (ref.50)	PEG (20) sorbitan monolaurate	98	95
Octylglucoside	12.6 (ref. 51)	Octyl-β-glucopyranoside	≤5	≤5
CHAPS	–	3-[3-cholamidopropyl)-dimethylammonio]-1-propanesuphonate	6	50

Lysates of prominin-transfected MDCK cells obtained using the indicated detergent (octylglucoside, 60 mM; CHAPS, 20 mM; all others, 0.5%) were centrifuged for 10 min at 17,000*g*, and the ER and plasma membrane (PM) form of prominin in the supernatant and pellet was quantitated by immunoblotting. Prominin in the pellet is expressed as percentage of total (sum of supernatant plus pellet); data are the mean of 3–6 experiments (except for Triton X-114 (*n=2*) and Tween 20 (*n=1*)). HLB, hydrophilic–lipophilic balance.

MDCK cells in which cell-surface prominin shows an apical-specific distribution[9] (data not shown). Cells were lysed in 0.5% Triton X-100 at 4 °C, and the lysates fractionated into supernatant and pellet and analysed by SDS–PAGE followed by immunoblotting for prominin. In prominin-transfected MDCK cells, prominin appears as two sets of immunoreactive bands of relative molecular mass (M_r) ~123,000 (123K) (Fig. 1a, b, brackets) and ~104K (Fig. 1a, b, asterisks)[9], which correspond to the endonuclease H (endoH)-resistant, microvillus-associated form and the endoH-sensitive, endoplasmic reticulum (ER) form of prominin, respectively[9]. After cell lysis in Triton X-100, both the cell-surface and the ER form of prominin were completely soluble after centrifugation for 10 min at 17,000*g* (Fig. 1a, lane 1) or 1 h at 100,000*g* (Fig. 1b, lane 1). The same results were obtained when the cells were lysed with a lower concentration of detergent (0.2% Triton X-100, data not shown).

Whereas insolubility of a membrane protein in Triton X-100 is consistent with it being associated with cholesterol–sphingolipid rafts, complete solubility in Triton X-100 does not exclude the possibility that it also engages in other, albeit Triton X-100-sensitive, horizontal interactions. We investigated whether using other detergents for solubilization might reveal such possible horizontal interactions involving prominin. Prominin-transfected MDCK cells were lysed at 4 °C with 0.5% Lubrol WX, another non-ionic detergent, and fractionated into supernatant and pellet. Upon centrifugation for 10 min at 17,000*g*, 43 ± 6% (n = 6) of the cell-surface form of prominin was sedimented (Fig. 1a, lanes 3, 4, bracket) whereas all of the ER form remained in the supernatant (Fig. 1a, lanes 3, 4, asterisk). Upon centrifugation for 1 h at 100,000*g*, all the cell-surface form (Fig. 1b, lanes 3, 4, bracket), but none of the ER form (Fig. 1b, lanes 3, 4, asterisk), of prominin was pelleted. The latter results suggested that the proportion of the cell-surface form that was recovered in the supernatant after centrifugation for 10 min at 17,000*g* (57%) was not truly soluble but reflected relatively small Lubrol WX-insoluble complexes. The same results were obtained when 1% or 3% Lubrol WX was used (data not shown).

Interestingly, comparison by Coomassie blue staining of the supernatants obtained after lysis in Triton X-100 or Lubrol WX and centrifugation for 10 min at 17,000*g* showed very similar total protein patterns, as did comparison of the pellets (Fig. 1c). Only a few proteins showed a differential distribution. One of them was completely sedimented upon lysis in Triton X-100 but not Lubrol WX (Fig. 1c, arrowheads), whereas two others were largely sedimented in Lubrol WX but not Triton X-100 (Fig. 1c, arrows). These observations suggested that the insolubility of cell-surface prominin in Lubrol WX was not due to an overall lower efficiency of Lubrol WX (compared to Triton X-100) as a detergent, but reflected a specific phenomenon.

Differential solubility of prominin in various detergents reflects their hydrophilic–lipophilic balance. To investigate whether the insolubility of cell-surface prominin in Lubrol WX is unique for this detergent, we examined others (Table 1). Upon lysis of prominin-transfected MDCK cells in non-ionic detergents such as Triton X-102, Brij 58 and the zwitterionic detergent CHAPS, the majority of the cell-surface prominin, but not the ER form, was sedimented upon centrifugation for 10 min at 17,000*g*, as found with Lubrol WX. With other non-ionic detergents, however, such as Triton X-114, Lubrol PX, Brij 56 and octylglucoside, very little of either form of prominin was found in the pellet, as with Triton X-100. We compared the structures of those detergents in which the cell-surface form of prominin was either largely absent from, or predominantly present in, the pellet and in which the ER form was always largely absent from the pellet, and which differ from each other only in the size of their polyethyleneglycol moiety, that is, the size of the polar headgroup (for example, Triton X-100 or Triton X-114 compared to Triton X-102; Brij 56 compared to Brij 58). This revealed that detergent insolubility of cell-surface prominin correlated with an increase in the size of the headgroup. In accordance with this, detergents with hydrophilic–lipophilic balance (HLB)[14,15] ≥ 14.6 led to the sedimentation of about half the cell-surface prominin at 17,000*g* whereas those with HLB ≤ 13.5 did not. Detergents with HLB ≥ 16.7, such as Brij 35 and Tween 20, resulted in the sedimentation of both cell-surface and ER prominin.

Insolubility of cell-surface prominin in Lubrol WX is not due to interaction with cytoskeletal elements. Insolubility of a membrane protein in detergents such as those listed in Table 1 can be due to its association with detergent-resistant lipid rafts and/or its anchoring to cytoskeletal elements. Octylglucoside is a mild detergent that is thought to preserve the cytoskeleton and its associated membrane proteins[16]. Hence, the lack of sedimentation of prominin in octylglucoside (Table 1) suggested that it was not tightly associated with the cytoskeleton. This in turn suggested that the insolubility of the cell-surface form of prominin in Lubrol WX was not due to cytoskeletal interactions. To investigate this directly, we repeated the lysis of cells in Lubrol WX (see Fig. 1) using buffers of high

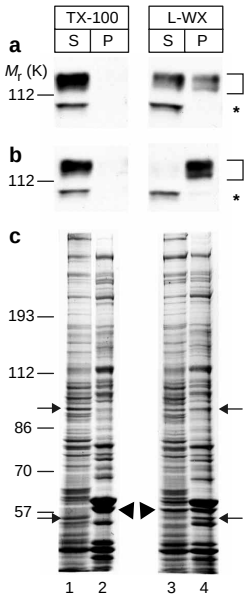

Figure 1 **Prominin is soluble in Triton X-100 but insoluble in Lubrol WX.** Prominin-transfected MDCK cells were lysed at 4 °C in 0.5% Triton X-100 (TX-100) or 0.5% Lubrol WX (L-WX) and centrifuged either for 10 min at 17,000*g* (**a, c**) or for 1 h at 100,000*g* (**b**). Supernatant (S) and pellet (P) were analysed by SDS–PAGE followed by either immunoblotting for prominin (**a, b**) or Coomassie blue staining (**c**). **a, b**, In this and all subsequent figures, a bracket denotes the cell-surface form of prominin, an asterisk, the ER form. **c**, Arrows, examples of proteins that are largely sedimented at 17,000*g* after lysis in Lubrol WX but not Triton X-100 (the 94 kDa band is the ER-resident protein calnexin); arrowheads, an example of a protein that is completely sedimented at 17,000*g* after lysis in Triton X-100 but not Lubrol WX.

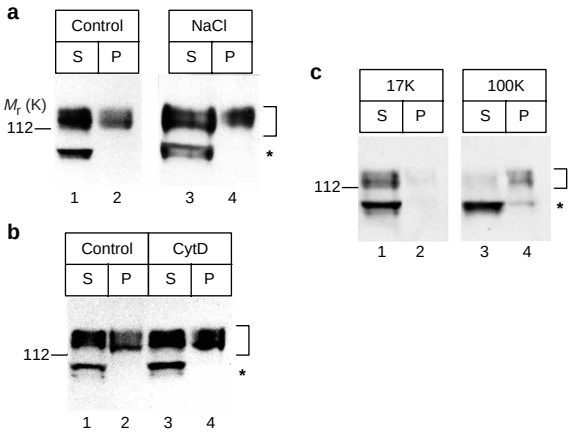

Figure 2 **Prominin's insolubility in Lubrol WX is not due to linkage to the actin cytoskeleton or other protein–protein interactions. a**, Prominin-transfected MDCK cells were lysed in 0.5% Lubrol WX at 4 °C in the absence (Control) or presence (NaCl) of 1 M sodium chloride. **b**, Prominin-transfected MDCK cells were incubated for 4 h at 37 °C in the absence (Control) or presence (CytD) of 1 μM cytochalasin D followed by lysis in 0.5% Lubrol WX at 4 °C. **c**, Prominin-transfected MDCK cells were lysed in 0.5% Lubrol WX at 37 °C. **a–c**, Cell lysates were centrifuged either for 10 min at 17,000*g* (17K) or for 1 h at 100,000*g* (**c**, 100K), and supernatant (S) and pellet (P) analysed by immunoblotting for prominin.

ionic strength, containing either 1 M NaCl (Fig. 2a, lanes 3, 4) or 250 mM $(NH_4)_2SO_4$ (data not shown). At this concentration, $(NH_4)_2SO_4$ has been reported to disrupt the cytoskeleton in MDCK cells[17]. In either condition, the proportion of cell-surface prominin recovered in the 17,000*g* pellet was the same as in low ionic strength buffer (Fig. 2a, lanes 1–4). Pretreatment of prominin-transfected MDCK cells with the actin-disrupting drug cytochalasin D (ref. 18) before lysis in Lubrol WX also did not decrease the insolubility of the cell-surface form of prominin (Fig. 2b, lanes 1–4). Together, these observations indicate that the insolubility of cell-surface prominin in Lubrol WX is not due to interaction with cytoskeletal elements.

Insolubility of cell-surface prominin in Lubrol WX reflects its association with detergent-resistant, floating complexes. When cells were lysed in Lubrol WX at 37 °C instead of 4 °C, most of the cell-surface form of prominin sedimented upon centrifugation for 1 h at 100,000*g* (Fig. 2c, lanes 3, 4) but was completely recovered in the supernatant after centrifugation for 10 min at 17,000*g* (Fig. 2c, lanes 1, 2). This lack of sedimentation at moderate centrifugal force is reminiscent of that reported for proteins associated with lipid rafts, for example, placental alkaline phosphatase (PLAP), in Triton X-100 (ref. 19). As higher temperatures enhance the lateral mobility of lipids in the bilayer and decrease their tendency to engage in horizontal interactions[20], our data raised the possibility that the insolubility of cell-surface prominin in Lubrol WX reflected its association with a novel type of lipid raft that is soluble in Triton X-100 but insoluble in Lubrol WX.

Membrane proteins associated with the Triton X-100-insoluble lipid raft float in a sucrose density gradient[19]. Thus, if cell-surface prominin is associated with a Lubrol WX-insoluble lipid raft, this prominin should also float in a sucrose density gradient. Indeed, when a Lubrol WX lysate of prominin-transfected MDCK cells was analysed using a flotation equilibrium sucrose density gradient, 10–30% of the cell-surface prominin (Fig. 3b, bracket), but none of the ER form (Fig. 3b, asterisk), floated to the low-density fractions 3–5. Flotation of prominin occurred irrespective of the absence (Fig. 3b) or presence (data not shown) of 0.1% Lubrol WX in the sucrose gradient and was also observed when cells were lysed at 1 mg (rather than 3.5 mg) protein per ml in 1% (rather than 0.5%) Lubrol WX (data not shown). The prominin floating to fractions 3–5 presumably corresponded to the prominin associated with the relatively large Lubrol WX-insoluble complexes sedimented after centrifugation for 10 min at 17,000*g* (Fig. 1a, lane 4, bracket). Consistent with this, no prominin was found to float to fractions 3–5 when cells were lysed in Triton X-100 (Fig. 3a), in line with prominin's complete solubility in this detergent (Fig. 1b, lanes 1, 2).

Upon solubilization in Triton X-100, both forms of prominin were recovered in the bottom fractions 7 and 8 of the flotation gradient (Fig. 3a), with fraction 8 corresponding to the load. These two fractions also contained the population of cell-surface prominin that did not float to fractions 3–5 upon cell lysis in Lubrol WX (Fig. 3b, bracket), as well as almost all of the ER form of the protein (Fig. 3b, asterisk). When fraction 7 from a Lubrol WX lysate was diluted and subjected to centrifugation for 1 h at 100,000*g*, cell-surface prominin was sedimented whereas the ER form remained in the supernatant (Fig. 3e). Hence, the flotation of prominin from fraction 8 to fraction 7 reflects two phenomena. The first is the association with detergent micelles of the detergent-soluble forms of prominin (ER form in Triton X-100 and Lubrol WX, cell-surface form in Triton X-100). The second is the association of the cell-surface form in Lubrol WX with a detergent-resistant complex of smaller size and greater buoyant density than that floating to fractions 3–5. Consistent with this interpretation, immunoreactivity for the transferrin receptor, a non-raft protein containing only one transmembrane domain, was predominantly detected in fraction 8, that is, the load (Fig. 3a, b).

In agreement with the conclusion that the insolubility of the cell-surface form of prominin in Lubrol WX is not due to its interaction with the actin cytoskeleton, the vast majority of actin was recovered in the load (fraction 8) and pellet of the gradient, the latter being virtually devoid of prominin (Fig. 3b), as was the case for gradients of Triton X-100 lysates (Fig. 3a).

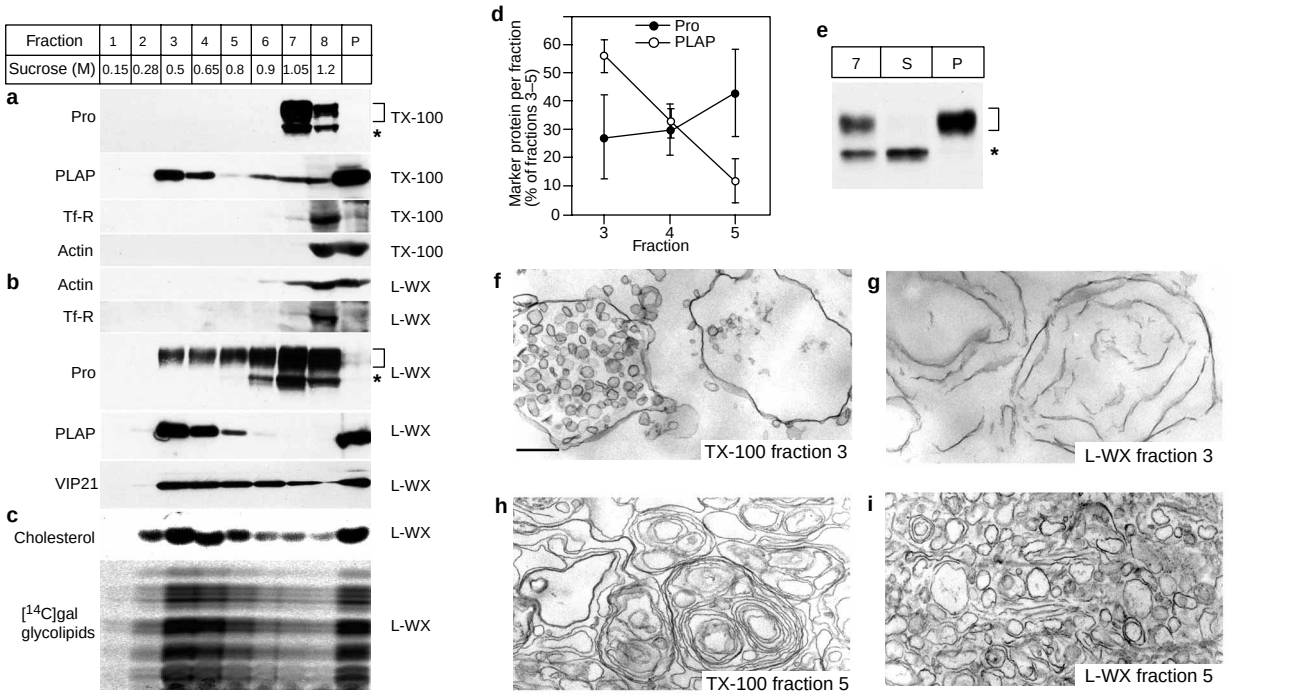

Figure 3 **Prominin's insolubility in Lubrol WX reflects its association with detergent-resistant complexes.** Unlabelled MDCK cells transfected with either prominin or PLAP, or prominin-transfected MDCK cells labelled for 20 h with [^{14}C]galactose, were lysed at 4 ˚C in either 0.5% Triton X-100 (TX-100, **a**) or 0.5% Lubrol WX (L-WX, **b–e**), the cell lysates were subjected to flotation on a sucrose density step gradient. The gradient fractions were analysed for prominin (Pro), PLAP, transferrin receptor (Tf-R), VIP21 and actin by immunoblotting (**a, b**) and for cholesterol and [^{14}C]galactose-containing glycolipids by TLC (**c**). The prominin and PLAP immunoblots in **b** are from cells that, before lysis in Lubrol WX, were incubated for 30 min at 4 ˚C in the absence of mβCD (controls for the immunoblots shown in Fig. 4b); this incubation did not affect the distribution of either protein across the gradient. **a–c**, Fraction 1, top of gradient; P, pellet. The average sucrose concentration in the fractions collected from at least five gradients is indicated. **d**, Quantification of prominin (filled circles) and PLAP (open circles) in fractions 3–5 of sucrose density gradients prepared after lysis in Lubrol WX. For each marker protein, the amount in a given fraction is expressed as percentage of the sum of fractions 3–5; data are the mean of 16 (Pro) and 5 (PLAP) gradients; bars, s.d. **e**, Fraction 7 of a gradient prepared after lysis in Lubrol WX was diluted, centrifuged for 1 h at 100,000*g*, and the supernatant (S) and pellet (P) as well as an aliquot of the undiluted fraction 7 (7) were analysed by immunoblotting for prominin. **f–i**, Electron microscopy of pellets obtained from fraction 3 (**f, g**, top of pellets) and 5 (**h, i**, bottom of pellets) of sucrose flotation gradients prepared after lysis in either Triton X-100 (**f, h**) or Lubrol WX (**g, i**). All panels are the same magnification; scale bar = 300 nm.

The low-density fractions 3–5 of the gradient contained the bulk of the cholesterol and galactoglycolipids present in the Lubrol WX lysate, whereas only small, but significant, amounts of these lipids (see Discussion) were found in the high-density fractions 6–8 (Fig. 3c). These data show that specific detergent-resistant complexes, which are not recovered upon lysis in Triton X-100, can be recovered upon lysis of cells in Lubrol WX. These complexes contain lipids that are also found in the Triton X-100-insoluble rafts, and certain proteins, notably prominin, that are not found in these rafts.

The detergent-resistant complexes containing prominin are distinct from those containing the GPI-anchored protein PLAP. The flotation gradient of the Lubrol WX cell lysate was further analysed for two membrane proteins known to be enriched in the Triton X-100-insoluble rafts and hence to float on a sucrose gradient[19]—PLAP (using PLAP-transfected MDCK cells[19]) (Fig. 3a), a GPI-anchored membrane protein, and VIP21/caveolin (endogenously present in MDCK cells[21,22]). Upon cell lysis in Lubrol WX, both proteins were found to float to the low-density fractions 3–5 (Fig. 3b). Interestingly, however, the distribution of PLAP in these fractions was distinct from that of prominin. PLAP was consistently highly enriched in fraction 3 compared with fractions 4 and 5 (Fig. 3d), whereas prominin was equally distributed across these three fractions (Fig. 3d). This is consistent with (at least some) prominin and PLAP being present in physically separate detergent-resistant complexes after cell lysis in Lubrol WX.

The particulate material floating to fractions 3 and 5 upon lysis of MDCK cells in either Lubrol WX or Triton X-100 was sedimented after dilution and the pellets were analysed by electron microscopy. The morphology of the Lubrol WX-resistant and the Triton X-100-resistant complexes was distinct. The Lubrol WX-resistant complexes observed at the bottom of the pellet obtained from fraction 5 (Fig. 3i) consisted of bilayered vesicular structures that were smaller and less frequently multilamellar than the Triton X-100-resistant complexes observed at the bottom of the fraction 5 pellet (Fig. 3h). A similar difference between Lubrol WX-resistant and Triton X-100-resistant complexes was found at the bottom of the fraction 3 pellets (data not shown). Striking differences between Lubrol WX-resistant and Triton X-100-resistant complexes were also observed at the top of the pellets, as shown for fraction 3 in which the Lubrol WX-resistant complexes often consisted of bilayered sheets (Fig. 3g) and the Triton X-100-resistant complexes of small vesicular structures (Fig. 3f).

The Lubrol WX-resistant complexes containing prominin are sensitive to cholesterol depletion. If prominin is associated with a Lubrol WX-resistant complex distinct from that containing PLAP, and given that cholesterol is enriched in the low-density fractions of the gradient containing this complex, the question arises whether cholesterol is needed to maintain its structure, as is the case for the Triton X-100-insoluble raft[23]. To remove cholesterol from the plasma membrane, prominin-transfected MDCK cells

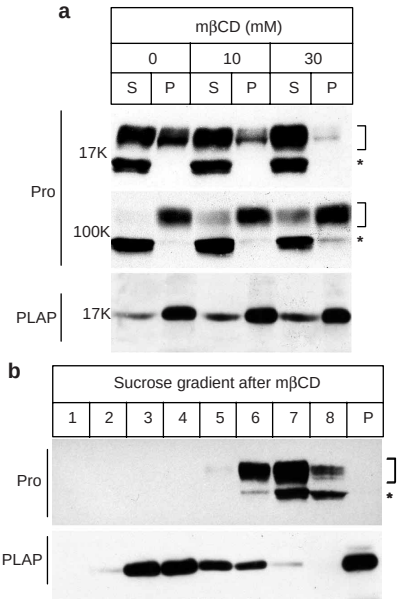

Figure 4 **Cholesterol depletion affects the Lubrol WX-resistant complexes containing prominin. a**, Prominin- or PLAP-transfected MDCK cells were treated for 30 min at 4 °C with the indicated concentrations of mβCD, lysed in 0.5% Lubrol WX, centrifuged either for 10 min at 17,000*g* (17K) or for 1 h at 100,000*g* (100K), and supernatant (S) and pellet (P) were analysed by immunoblotting for prominin (Pro) and PLAP. **b**, Prominin- or PLAP-transfected MDCK cells were treated for 30 min at 4 °C with 50 mM mβCD, lysed in 0.5% Lubrol WX, subjected to flotation on a sucrose density step gradient, and the gradient fractions were analysed by immunoblotting for prominin (Pro) and PLAP. The controls, that is cells treated without mβCD, are shown in Fig. 3b.

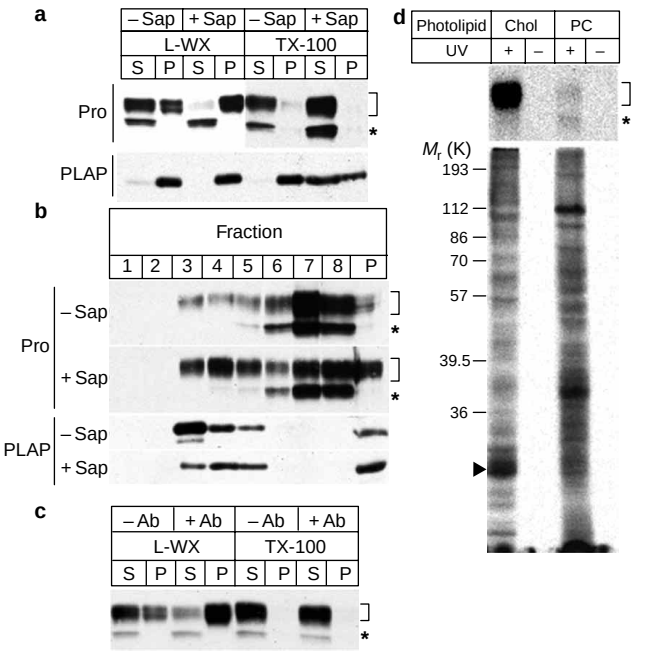

Figure 5 **Clustering of either cholesterol or prominin increases the size of the Lubrol WX-insoluble, prominin-containing complexes. a, b**, Prominin- or PLAP-transfected MDCK cells were treated for 30 min at 4 °C without (– Sap) or with (+ Sap) 0.2% saponin, lysed in either 0.5% Lubrol WX (L-WX) or Triton X-100 (TX-100), and either centrifuged for 10 min at 17,000*g* (**a**) or subjected to flotation on a sucrose density step gradient (**b**). Supernatant (S) and pellet (P) (**a**) and gradient fractions (**b**) were analysed by immunoblotting for prominin (Pro) and PLAP. **c**, Prominin-transfected MDCK cells were incubated for 1 h at 37 °C without (– Ab) or with (+ Ab) the anti-prominin monoclonal antibody 13A4, lysed in either 0.5% Lubrol WX (L-WX) or Triton X-100 (TX-100), centrifuged for 10 min at 17,000*g*, and supernatant (S) and pellet (P) were analysed by immunoblotting for prominin. **d**, Prominin-transfected MDCK cells were incubated for 15 h in the presence of [^{3}H]photo-cholesterol (Chol) or 10-azi stearic acid plus [^{3}H]choline to generate photo-phosphatidylcholine (PC), subjected to UV irradiation (+) or kept in the dark (–). The total detergent extract of the cells (bottom panel of gel) and prominin immunoprecipitated therefrom (top panel of gel) were analysed by SDS–PAGE followed by phosphoimaging. Arrowhead, caveolin.

were treated at 4 °C with methyl-β-cyclodextrin (mβCD), which is known to selectively deplete biological membranes of cholesterol[24]. Upon treatment of scraped cells with 30 mM and 50 mM mβCD, total cellular cholesterol was reduced by 30% and 47%, respectively (data not shown). This mβCD treatment *per se* did not lead to the solubilization of prominin (data not shown). When prominin- or PLAP-transfected MDCK cells were treated at 4 °C with 10 mM or 30 mM mβCD and subsequently lysed in Lubrol WX, most and virtually all of the cell-surface form of prominin, respectively, remained in the supernatant upon centrifugation for 10 min at 17,000*g* (Fig. 4a, Pro 17K, bracket). This is in contrast to PLAP, most of which was still sedimented under these conditions (Fig. 4a, PLAP 17K). This lack of sedimentation of cell-surface prominin, in contrast to that of the ER form (Fig. 4a, Pro 17K, asterisk), did not reflect true solubility upon cholesterol depletion (using up to 30 mM mβCD) because the majority of the cell-surface form (Fig. 4a, Pro 100K, bracket), but virtually none of the ER form (Fig. 4a, Pro 100K, asterisk), was sedimented upon centrifugation for 1 h at 100,000*g*.

When prominin-transfected MDCK cells, before lysis in Lubrol WX, were treated at 4 °C with 50 mM mβCD, about half of the cell-surface prominin was soluble upon centrifugation for 1 h at 100,000*g* (data not shown). Flotation gradient analysis of a Lubrol WX lysate revealed that the mβCD treatment altered the flotation behaviour of the cell-surface prominin, but not that of the ER form. Instead of a proportion of cell-surface prominin floating to the low-density fractions 3–5, almost all of it floated from fraction 8 (the load) to fractions 7 and 6 (Fig. 4b, Pro, bracket; compare Fig. 3b, Pro, bracket). In contrast, flotation gradient analysis of a similar Lubrol WX lysate from PLAP-transfected cells revealed that the mβCD treatment shifted the peak of floating PLAP by only approximately one fraction towards higher density (Fig. 4b, PLAP; compare Fig. 3b, PLAP). Hence, the conditions of mβCD treatment used here (30–50 mM mβCD for 30 min at 4 °C), though not resulting in the complete solubilization of either prominin or PLAP in Lubrol WX (Fig. 4a), affected the detergent-resistant prominin much more than PLAP. The prominin-containing detergent-resistant complexes decreased in size (no longer sedimenting at 17,000*g* but still at 100,000*g*; Fig. 4a) and increased in buoyant density (floating to fractions 6 and 7 rather than 3–5; Fig. 4b). Our conditions of mβCD treatment appear to be milder than those used by others (for example, 10 mM mβCD for 30 min at 37 °C in ref. 23), in which PLAP was rendered completely soluble upon cell lysis in 1% Triton X-100.

The detergent-resistant complexes containing prominin and PLAP are differentially affected by cholesterol clustering. Further evidence for the existence of two distinct, but nonetheless cholesterol-dependent, detergent-resistant complexes containing either prominin or PLAP was obtained when prominin- and PLAP-transfected MDCK cells were treated with a low concentration of saponin (0.2%) before detergent lysis. At such a low concentration, saponin does not extract cholesterol from membranes (data not shown)[25], but is thought to cause its clustering in the membrane[25]. Upon saponin pretreatment of cells that were then lysed in Lubrol WX,

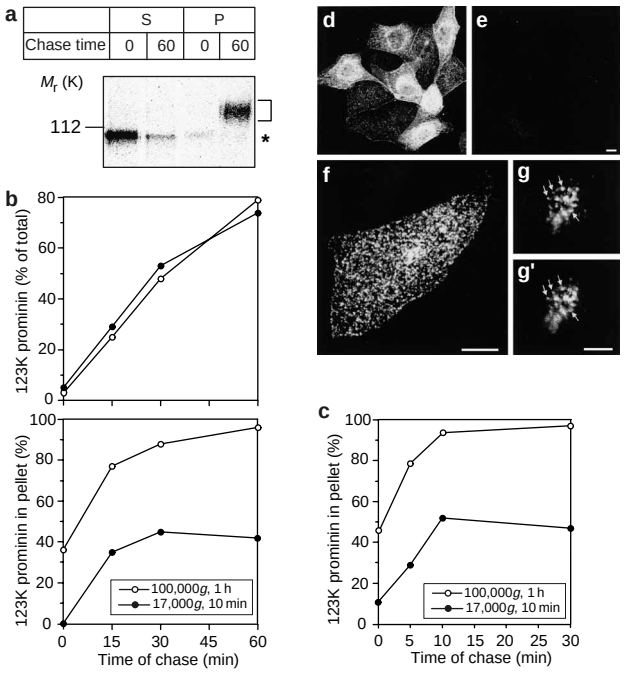

Figure 6 **Prominin becomes insoluble in Lubrol WX within the *trans*-Golgi/TGN, and the size of the detergent-resistant complexes increases upon exit from the TGN. a–b**, Prominin-transfected MDCK cells were pulse-labelled for 20 min with [^{35}S]methionine/cysteine, chased for the indicated periods of time (min), lysed in 0.5% Lubrol WX, centrifuged either for 10 min at 17,000*g* (filled circles) or for 1 h at 100,000*g* (open circles), and prominin was immunoprecipitated from the supernatant (S) and pellet (P) and analysed by SDS–PAGE followed by phosphoimaging. **a**, Autoradiogram of the 0 and 60 min chase condition (100,000*g* centrifugation); bracket, TGN and plasma membrane form of prominin; asterisk, ER and early Golgi form of prominin. **b**, Top panel, time course of appearance of the TGN and plasma membrane form of prominin. For each time point and condition of centrifugation, the TGN/plasma membrane form in the sum of supernatant plus pellet is expressed as percentage of total prominin (sums of ER/early Golgi plus TGN/plasma membrane forms in supernatant plus pellet). Bottom panel, time course of acquisition of detergent-insolubility of the TGN and plasma membrane form of prominin. For each time point and condition of centrifugation, the TGN/plasma membrane form in the pellet is expressed as percentage of total TGN/plasma membrane form (sum of pellet plus supernatant). **c**, Prominin-transfected MDCK cells were pulse-labelled for 5 min with [^{35}S]sulphate, chased for the indicated time periods and processed as in a-b. For each time point and condition of centrifugation, prominin in the pellet is expressed as percentage of total (sum of pellet plus supernatant). **d–g′**, Prominin-transfected MDCK cells were extracted four times for 5 s at room temperature with 0.5% Lubrol WX (**d, f–g′**) or 0.5% Triton X-100 (**e**), fixed with paraformaldehyde, and analysed for prominin by immunofluorescence (**d–g**) and for F-actin by TRITC-phalloidin fluorescence (**g′**) using confocal microscopy. **d, e**, Overview comparing the extraction of prominin with Lubrol WX (**d**) and Triton X-100 (**e**); each picture is a composite of four optical sections through the cells, obtained with identical confocal settings. **f**, Representative pattern of prominin immunofluorescence at the apical side of the cell; composite picture of nine optical sections. **g, g′**, High-magnification view of a single optical section at the level of the apex of the cell in **f**, showing co-localization (arrows) of prominin immunofluorescence (**g**) with F-actin as revealed by TRITC–phalloidin fluorescence (**g′**). Scale bars = 10 μm (**e, f**); 5 μm (**g′**).

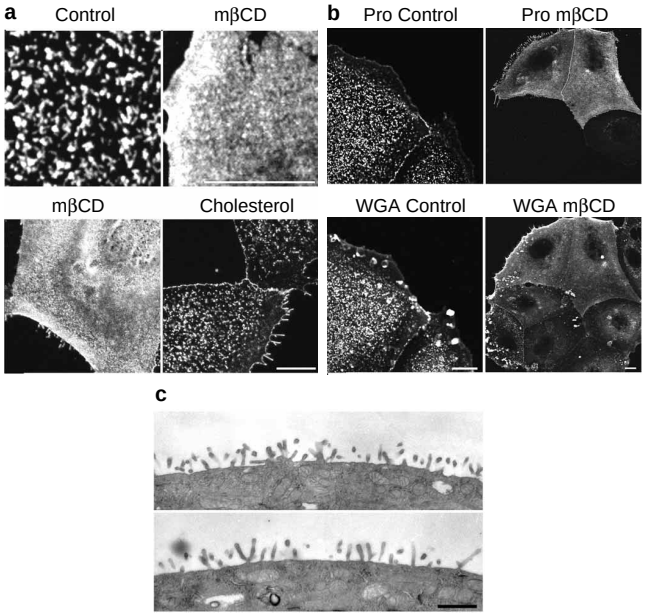

Figure 7 **The characteristic microvillus-specific pattern of prominin's cell-surface distribution depends on cholesterol. a**, Effect of cholesterol depletion and replenishment. Top panels (equal magnification), prominin-transfected MDCK cells were incubated for 30 min at 4 °C in the absence (Control) or presence (mβCD) of 50 mM mβCD and analysed by cell-surface immunofluorescence for prominin using confocal microscopy. Single optical sections at the level of the apex of the cells are shown. Bottom panels (equal maginification), effect of cholesterol replenishment. Prominin-transfected MDCK cells incubated for 30 min at 4 °C with 50 mM mβCD in Ca/Mg-PBS were either kept for 1 h at 4 °C in Ca/Mg-PBS without mβCD (mβCD) or incubated for 1 h at 37 °C in E-MEM supplemented with 10% delipidated serum and containing 2.5 mg ml^{-1} mβCD–cholesterol complex (Cholesterol), and analysed by cell-surface immunofluorescence for prominin using confocal microscopy. Composite pictures of four optical sections are shown. Scale bars = 10 μm. **b**, Comparison of prominin and wheat germ agglutinin (WGA) cell-surface fluorescence. Prominin-transfected MDCK cells were incubated for 30 min at 4 °C in the absence (Control) or presence (mβCD) of 50 mM mβCD and analysed by cell-surface double (immuno)fluorescence for prominin (Pro) and WGA using confocal microscopy. Single optical sections at the level of the dorsal plasma membrane are shown. The right panels are a lower magnification than the left panels; scale bars = 10 μm. **c**, Morphology of microvilli. Prominin-transfected MDCK cells were incubated for 30 min at 4 °C in the absence (top) or presence (bottom) of 50 mM mβCD and analysed by electron microscopy. The electron micrographs shown are representative of at least 15 cells. Scale bar = 500 nm.

sedimentation of cell-surface prominin at 17,000*g* was drastically increased (Fig. 5a). In contrast, prominin's complete recovery in the supernatant upon cell lysis in Triton X-100 was unchanged by saponin pretreatment (Fig. 5a). Conversely, PLAP, which was reported to be increasingly recovered in the supernatant upon saponin pretreatment of cells followed by cell lysis in Triton X-100 (ref. 25), an observation confirmed here (Fig. 5a), remained completely insoluble in Lubrol WX after saponin pretreatment (Fig. 5a). Consistent with these observations, a greater proportion of the cell-surface form of prominin was found in fractions 3–5 of the sucrose flotation gradient after saponin pretreatment followed by lysis in Lubrol WX (Fig. 5b). In contrast, for PLAP, the peak of the floating material shifted from fraction 3 by about one fraction towards higher density (Fig. 5b). Hence, saponin seems to affect distinct pools of cholesterol whose clustering has pronounced and differential effects on the detergent-resistant complexes containing either of the proteins.

Antibody binding to cell-surface prominin results in crosslinking of Lubrol WX-insoluble complexes. Antibody-induced crosslinking of membrane proteins associated with Triton X-100-insoluble rafts is thought to result in clustering of the rafts themselves[26]. In the light of this observation, we pretreated prominin-transfected

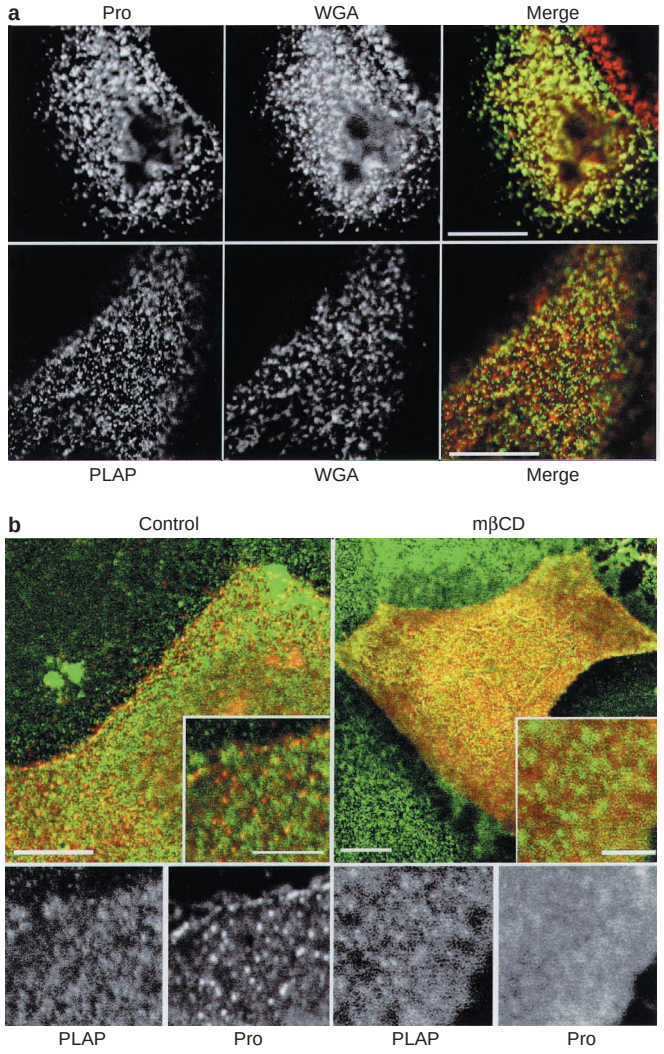

Figure 8 **PLAP does not co-localize with prominin on microvilli and does not redistribute like prominin upon cholesterol depletion. a**, MDCK cells stably expressing prominin (top row) or PLAP (bottom row) were subjected to double cell-surface labelling using either anti-prominin (Pro) or anti-PLAP (PLAP) antibody (left panels) plus WGA (centre panels), fixed with paraformaldehyde, and analysed by double fluorescence using confocal microscopy. Single optical sections are shown. Prominin, green; WGA, red in top merge panel; PLAP, green; WGA, red in bottom merge panel. Scale bars = 10 μm. **b**, MDCK cells stably expressing PLAP and transiently transfected with prominin were incubated for 30 min at 4 °C without (Control) or with 50 mM mβCD (mβCD), fixed with paraformaldehyde/methanol and analysed by double immunofluorescence for PLAP (green) and prominin (red) using confocal microscopy. Single optical sections are shown. The panels in the bottom row show the individual scans for PLAP and prominin (Pro) that are merged in the insets in the upper panels. Scale bars = 10 μm; scale bars in insets = 5 μm.

MDCK cells at 37 °C with the monoclonal antibody 13A4, which is directed against the extracellular domain of prominin, and then lysed the cells in either Lubrol WX or Triton X-100 at 4 °C. Addition of antibody greatly increased sedimentation of the cell-surface form of prominin at 17,000*g* upon subsequent cell lysis in Lubrol WX (Fig. 5c). It did not, however, alter its lack of sedimentation after lysis in Triton X-100 (Fig. 5c).

Cell-surface prominin interacts directly with cholesterol. Given the observations described above, we investigated whether prominin interacts directly with cholesterol. We incubated prominin-transfected MDCK cells with [^{3}H]photocholesterol, a photoactivatable radioactive derivative of cholesterol[27], and compared the labelling obtained upon ultraviolet (UV) irradiation with that obtained after incubation of cells with 10-azi stearic acid plus [^{3}H]choline, which leads to the intracellular generation of a photoactivatable radioactive phosphatidylcholine (PC)[27]. Analysis of the total cell lysate showed that, under our conditions, the overall amount of labelling of proteins by either [^{3}H]photocholesterol or [^{3}H]photo-PC was similar, with the cholesterol-interacting protein caveolin being strongly labelled by [^{3}H]photocholesterol but not [^{3}H]photo-PC (Fig. 5d, arrowhead), as reported previously[27]. Comparison of prominin immunoprecipitated from the lysates of [^{3}H]photocholesterol- and [^{3}H]photo-PC-labelled cells showed that the cell-surface form, but not the ER form, was specifically labelled by [^{3}H]photocholesterol (Fig. 5d). This indicated that cell-surface prominin and cholesterol directly and specifically interact with each other.

The detergent-resistant complexes containing prominin are assembled in the TGN. The cholesterol content of membranes in the secretory pathway increases continuously from the ER to the plasma membrane[28]. The Triton X-100-insoluble raft is already found in TGN-derived secretory vesicles[29]. We determined whether the prominin-containing Lubrol WX-insoluble complexes are formed in the TGN or at the plasma membrane. [^{35}S]Methionine/cysteine pulse-chase analysis of prominin-transfected MDCK cells showed that after a 20-min pulse, the 104K ER form of prominin (Fig. 6a, asterisk) was converted to the 123K cell-surface form (Fig. 6a, bracket) with a $t_{1/2}$ of ≈30 min (Fig. 6b, upper panel). Because the appearance of [^{35}S]methionine/cysteine-labelled prominin at the MDCK cell surface requires >30 min of chase (see Fig. 5 in ref. 9), conversion of the 104K form to the 123K form occurred before its arrival at the cell surface, most likely in the TGN. Centrifugation of the Lubrol WX lysate for 1 h at 100,000*g* revealed that the 104K form of prominin, which is known to be sensitive to endoH[9], remained soluble throughout its passage from the ER to, and through, the early Golgi complex (Fig. 6a, asterisk). In contrast, the 123K form of prominin, which is known to be endoH-resistant[9], became almost completely insoluble in Lubrol WX soon after it appeared, that is after 15 min of chase (Fig. 6a, bracket, and b, lower panel open circles). At this time, newly synthesized prominin has not yet arrived at the cell surface (see Fig. 5 in ref. 9).

The observation that prominin acquired insolubility in Lubrol WX before its arrival at the cell surface raised the following question. Were the detergent-resistant prominin-containing complexes only those that required centrifugation at 100,000*g* for sedimentation and floated to fractions 6 and 7 of the sucrose density gradient, or did they include those that sedimented at 17,000*g* (for 10 min) and floated to the low-density fractions 3–5? The latter was found to be the case (Fig. 6b, lower panel, filled circles).

Sulphation of membrane and secretory proteins on carbohydrate and/or tyrosine residues occurs in the TGN[30] and has been used to study transport of proteins from TGN to plasma membrane[31]. As prominin is sulphated on carbohydrate residues[8], we used [^{35}S]sulphate pulse-chase analysis of prominin-transfected MDCK cells to determine the exact intracellular site at which prominin becomes insoluble in Lubrol WX. Centrifugation for 1 h at 100,000*g* revealed that about half of the [^{35}S]sulphate-labelled prominin had acquired insolubility in Lubrol WX by the end of the 5 min [^{35}S]sulphate pulse (Fig. 6c). Interestingly, the kinetics of formation of the larger Lubrol WX-insoluble complexes, that is, those that were sedimented already by centrifugation for 10 min at 17,000*g*, were slower, showing a $t_{1/2}$ of ≈4 min (Fig. 6c). Remarkably, this value is identical to that previously reported for the formation of constitutive secretory vesicles from the TGN using the same pulse-chase protocol[32]. We conclude that prominin becomes part of relatively small Lubrol WX-insoluble complexes in the *trans*-Golgi/TGN and that these complexes cluster concomitantly with

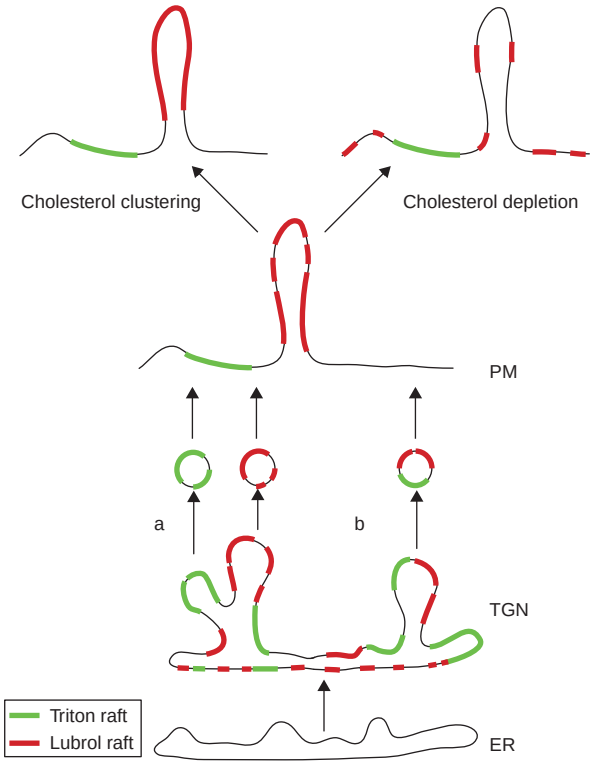

Figure 9 **Formation of the Triton rafts and Lubrol rafts in the TGN and their transport to the planar and the microvillar subdomains of the apical plasma membrane, as revealed after cell lysis in Lubrol WX.** Triton and Lubrol rafts are absent from the endoplasmic reticulum (ER) and assembled in the TGN, with the small type of Lubrol-rafts coalescing into the large type concomitantly with vesicle formation. Green membrane segments, Triton rafts; small and large red membrane segments, small and large types, respectively, of Lubrol rafts. Triton rafts and Lubrol rafts are delivered to the apical plasma membrane (PM) either separately in two distinct transport vesicles (**a**) or together in one common transport vesicle (**b**). Cholesterol clustering caused by saponin treatment promotes coalescence of the small type Lubrol rafts into the large type; cholesterol depletion caused by mβCD results in the dissociation of the large type into the small type, which is no longer retained in the microvillar subdomain.

the formation of apically destined, constitutive carrier vesicles from the TGN.

The detergent-resistant, cell-surface form of prominin is associated with microvilli. As cell-surface prominin is specifically associated with microvilli[8,9] and the cell-surface form of prominin is insoluble in Lubrol WX, one would expect the microvillus-associated form of prominin to be associated with the Lubrol WX-insoluble complexes. To examine this directly, prominin-transfected MDCK cells were briefly treated with Lubrol WX before fixation. Immunofluorescence of Lubrol WX-extracted cells showed that a significant proportion of prominin remained with the cells (Fig. 6, d,f), in a punctate pattern indistinguishable from that of cells not exposed to detergent (data not shown). In contrast, treatment of cells with Triton X-100 before fixation led to the loss of prominin immunofluorescence (Fig. 6e). Double confocal microscopy showed that the punctate prominin immunoreactivity after Lubrol WX treatment was co-localized with apical F-actin (Fig. 6, g, g′, arrows), indicating that Lubrol WX-insoluble prominin was associated with microvilli.

The microvillus-specific localization of prominin requires cholesterol. We then examined the effect of depleting cholesterol from the plasma membrane on the microvillus-specific localization of prominin. Prominin-transfected MDCK cells were depleted of plasma membrane cholesterol by adding 50 mM mβCD for 30 min at 4 °C and analysed for prominin cell-surface immunofluorescence by confocal microscopy. Remarkably, the punctate staining pattern of prominin (Fig. 7a, control), which reflects its specific localization in microvilli[9], was lost upon mβCD treatment, with prominin immunoreactivity becoming more evenly distributed over the cell surface (Fig. 7a, mβCD). The effect of mβCD treatment was reversible, as prominin regained its characteristic microvillus-specific localization when cholesterol was replenished by addition of a cholesterol-saturated mβCD complex to the cells for 1 h at 37 °C (Fig. 7a, cholesterol). Thus, the specific localization of cell-surface prominin in microvilli depends on an appropriate cholesterol content of the plasma membrane.

The puncta of prominin cell-surface immunofluorescence largely coincided with those observed upon cell-surface staining using wheat germ agglutinin (WGA) (Fig. 7b, Pro control and WGA control). This allowed us to examine whether only prominin lost its microvillus-specific localization after depletion of plasma membrane cholesterol (Fig. 7b, pro mβCD). Cell-surface WGA staining revealed that this loss was also observed for the bulk of the microvillar glycoproteins and glycolipids (Fig. 7b, WGA mβCD). Electron microscopy showed that cholesterol depletion did not significantly reduce the number and morphology of the microvilli (Fig. 7c). This is in line with observations by others made after short-term mβCD treatment[33], indicating that the loss of the microvillus-specific localization of prominin and other glycosylated membrane constituents was not due to a loss of microvilli as such.

Cholesterol-dependent localization of prominin in microvilli reflects a microdomain distinct from that containing PLAP. The differential solubility and flotation behaviour of two apical membrane proteins, prominin and PLAP, upon lysis of cells (with or without prior manipulation of cholesterol) in Lubrol WX compared to Triton X-100, together with the selective presence of prominin within the microvillar subdomains of the apical plasma membrane, raised the possibility that prominin and PLAP are each associated with distinct, spatially segregated lipid microdomains in the apical plasma membrane. We therefore subjected prominin-transfected MDCK cells and PLAP-transfected MDCK cells to double cell-surface labelling by incubation at 4 °C with fluorescently labelled WGA and either monoclonal anti-prominin or anti-PLAP antibody. Cells were fixed with paraformaldehyde and compared for the pattern of cell-surface immunofluorescence of prominin and PLAP, using the WGA staining as internal reference. Compared to the largely concident punctate patterns of prominin cell-surface immunofluorescence and WGA cell-surface staining (Fig. 8a, upper panels), the majority of PLAP cell-surface immunofluorescence rarely coincided with the WGA cell-surface staining (Fig. 8a, lower panels). The PLAP cell-surface immunofluorescence was also punctate, as previously described for antibody-patched PLAP[26], but the individual puncta were finer than in the case of prominin and WGA.

It was important to exclude the possibility that this differential cell-surface localization was due to either a differential effect on the cells expressing either prominin or PLAP, and/or the addition of the antibodies before paraformaldehyde fixation (although at 4 °C). We therefore expressed both proteins in the same cell (MDCK cells stably expressing PLAP and transiently transfected with prominin) and analysed their steady-state distribution by double immunofluorescence after paraformaldehyde/methanol fixation. Under these experimental conditions, the pattern of immunoreactivity for PLAP was distinct from that for prominin (Fig. 8b, control). Compared with the results from cell-surface immunolabelling before paraformaldehyde fixation (Fig 8a), PLAP immunolabelling after paraformaldehyde/methanol fixation, studied at the apex of the MDCK cells by confocal microscopy, was more diffuse (Fig. 8b, control), consistent with previous observations with PLAP-transfected BHK cells using comparable conditions of fixation[26].

Given the redistribution of prominin cell-surface immunofluorescence upon extraction of cholesterol from the plasma membrane (Fig. 7a), it was of interest to investigate the effect of this treatment on the differential localization of prominin versus PLAP at the apex of paraformaldehyde/methanol-fixed MDCK cells expressing both proteins. Remarkably, the staining pattern for PLAP did not change significantly upon treatment with 50 mM mβCD for 30 min at 4 °C (Fig. 8b, mβCD). As observed using cell-surface immunolabelling of prominin before paraformaldehyde fixation (Figs 7, 8a), prominin immunostaining after paraformaldehyde/methanol fixation changed from a punctate to a largely diffuse pattern after cholesterol extraction from the plasma membrane (Fig. 8b, mβCD). Interestingly, the pattern of prominin and PLAP staining observed upon mβCD treatment still did not fully coincide (Fig. 8b, mβCD). Together, these observations indicate that prominin, which is confined to microvilli, is present in a membrane microdomain that is spatially distinct from, and more sensitive to cholesterol removal than, that containing PLAP.

Discussion

Our study provides morphological evidence that two plasma membrane proteins—the polytopic membrane protein prominin[8,9] and the GPI-anchored protein PLAP[19,34]—which show an apical-specific localization when expressed in polarized epithelial cells, are spatially segregated within the apical plasma membrane of MDCK cells. Biochemical evidence shows that the solubility or insolubility of these two proteins differs in two distinct non-ionic detergents, Triton X-100 and Lubrol WX, and that the properties of the detergent-resistant complexes containing either protein are differentially affected by specific manipulations of plasma membrane cholesterol. We conclude that prominin and PLAP reside in distinct plasma membrane microdomains which differ in their protein–lipid interactions.

Ignoring the morphological data and considering the biochemical data alone, it could be argued that prominin and PLAP are present in the same membrane microdomain and that their differential behaviour upon detergent lysis simply reflects differences in their interaction with certain lipids and/or other proteins of this microdomain. One might propose that prominin interacts less strongly with sphingolipid–cholesterol rafts than PLAP; accordingly, Triton X-100, but not Lubrol WX, can solubilize prominin, whereas neither detergent can solubilize PLAP. If this were the case, one would expect that upon cell lysis in Lubrol WX, prominin and PLAP should be recovered in the same detergent-resistant complexes. However, the distribution of the prominin-containing and the PLAP-containing Lubrol WX-resistant complexes across the flotation gradient was distinct (Fig. 3d). In addition, if prominin and PLAP were present in the same membrane microdomain, the manipulation of plasma membrane cholesterol by low concentrations of saponin should affect the detergent-resistant complexes containing prominin and PLAP in a similar manner. Saponin pretreatment, however, increased the sedimentation and decreased the buoyant density of the Lubrol WX-resistant complexes containing prominin whereas it decreased the sedimentation and increased the buoyant density of the Triton X-100-resistant complexes containing PLAP (Fig. 5a, b). The latter argument against prominin and PLAP being constituents of the same membrane microdomain could be countered by proposing that PLAP, a GPI-anchored protein, is more sensitive to manipulation of plasma membrane cholesterol than the five-transmembrane domain protein prominin. But the opposite was observed, as limited extraction of plasma membrane cholesterol using mβCD at 4 °C had a marked effect on the size (reduction) and buoyant density (increase) of the Lubrol WX-resistant complexes containing prominin, but barely affected those containing PLAP (Fig. 4).

The morphological evidence shows that, irrespective of the mode of fixation and the addition of antibody either before or after fixation, most of the prominin and PLAP within the apical plasma membrane reside in spatially segregated subdomains (Fig. 8). Confirming previous observations[8,9], the prominin-containing subdomain is the microvillar portion of the apical plasma membrane, with the planar portion being essentially devoid of prominin. As prominin is found in most, if not all, microvilli, and PLAP is spatially segregated from prominin, it follows that the PLAP-containing subdomain of the apical plasma membrane corresponds to the non-microvillar, planar, portion (though not necessarily to all of it) (Fig. 9). Consistent with this, another GPI-linked protein that is insoluble in Triton X-100, the 80K iron-binding protein, was found to be largely excluded from the microvillar subdomains of the apical surface of intestinal epithelial cells and detected in its planar subdomains[35]. Some PLAP has been observed on microvilli of MDCK cells upon antibody-induced clustering before fixation[36]; it is unclear, however, whether this localization is in contrast to our findings or the result of the clustering.

The localization of prominin and PLAP in distinct subdomains of the apical plasma membrane explains why these two proteins are largely recovered in physically separate detergent-resistant complexes upon cell lysis in Lubrol WX. Moreover, it is interesting to note that our biochemical findings on the detergent solubility/insolubility of prominin and PLAP under various conditions match our morphological observations on the distribution of prominin and PLAP within the apical plasma membrane. First, both the characteristic, microvillus-specific cell-surface staining for prominin (Fig. 6, d–g′) and its insolubility upon detergent lysis of cells (Fig. 1) was preserved in Lubrol WX but abolished in Triton X-100. Second, limited extraction of plasma membrane cholesterol resulted in prominin losing both its microvillus-specific cell-surface staining (Fig. 7) and its association with the 'large' type (sedimented at 17,000*g*, see below) of Lubrol WX-resistant complexes (Fig. 4). But it had no effect on the cell-surface distribution of PLAP (Fig. 8b) and the properties of the Lubrol WX-resistant complexes containing PLAP (Fig. 4).

We therefore conclude that the differences between prominin and PLAP regarding their solubility in Triton X-100 (Figs 1, 3a), the changes in the properties of the detergent-resistant complexes upon cholesterol extraction by mβCD (Fig. 4) and manipulation of cholesterol by saponin (Fig. 5a, b), and the redistribution at the cell surface upon cholesterol extraction (Figs 7, 8b), indicate that the protein–lipid interactions, notably those involving cholesterol, in the microvillar and planar subdomains of the apical plasma membrane are different. We propose that there are multiple, distinct types of raft-like assemblies of lipids and proteins, which can coexist within one biological membrane (Fig. 9). Importantly, our data demonstrate that different detergents (characterized, for example, by different HLB values; Table 1) may be required to reveal distinct types of rafts. In this context, it is interesting to note that the electron microscopic appearance of the Triton X-100-resistant and the Lubrol WX-resistant complexes obtained from whole-cell lysates was distinct (Fig. 3e–h). We will use the operational term 'Triton raft' for the detergent-resistant complexes that are insoluble (sedimented upon centrifugation for 1 h at 100,000*g* and 4 °C) in both Triton X-100 and Lubrol WX, with PLAP being a marker of this raft but not required for its formation. We will use the term 'Lubrol-raft' for the detergent-resistant complexes that are soluble in Triton X-100 but insoluble in Lubrol WX upon centrifugation for 1 h at 100,000*g* and 4 °C, with prominin being a marker of this raft, but not required for its formation.

The coexistence in one membrane of distinct types of rafts with differential sensitivity to various detergents may explain some of the previously reported differences in the extent of detergent insolubility of various plasma membrane proteins[37–39]. Our proposal of the coexistence of distinct types of rafts is obviously not restricted to the apical plasma membrane studied here, nor to epithelial cells. In this context, prominin, when expressed in non-epithelial cells, is also selectively localized in plasma membrane protrusions and is

absent from the planar regions of the cell surface[8], and its cell-surface distribution in non-epithelial cells is also affected by cholesterol extraction (K.R., D.C. and W.B.H., unpublished data).

It is currently unknown whether the distinct types of raft-like assemblies of lipids and proteins in the apical plasma membrane of MDCK cells that we propose here differ in their lipid composition, the organization of lipid–lipid and lipid–protein interactions, or both. Observations of another membrane organelle, the synaptic vesicle, may be instructive in this regard. The synaptic vesicle, which is rich in cholesterol but low in sphingolipids[40], is recycled from the presynaptic plasma membrane, which is rich in both of these raft lipids[41]. It has been proposed that synaptic-vesicle formation from the plasma membrane involves the interaction of cholesterol with synaptophysin, a four-transmembrane domain protein with an affinity for cholesterol[27]. It may be more than a coincidence that synaptophysin, like prominin, is completely soluble in Triton X-100 but not in Lubrol WX (M.J. Hannah and W.B.H., unpublished data), and that prominin, like synaptophysin[27], specifically interacts with cholesterol *in vivo* (Fig. 5d).

Whatever the precise organization of the microvillar plasma membrane subdomain, our data indicate that the cholesterol in this membrane, rather than the submembraneous actin cytoskeleton, has a key role in the retention of prominin and other, WGA-binding, constituents in this subdomain. Limited extraction of cholesterol from the plasma membrane resulted in the loss of the microvillus-specific localization of cell-surface prominin and of the predominantly microvillar cell-surface WGA staining, without abolishing the microvilli as such (Fig. 7) or the F-actin staining characteristic of microvilli (data not shown). Conversely, in contrast to the effects of cholesterol depletion (Fig. 4), treatments known to disrupt the actin cytoskeleton and its interaction with membranes did not reverse the association of prominin with the Lubrol WX-resistant complexes (Fig. 2). Very little, if any, actin was associated with these complexes even without such treatments (Fig. 3b). Furthermore, on cytochalasin D treatment of prominin-transfected MDCK cells and in Caco2 cells expressing a villin antisense cDNA[42], cell-surface prominin was still confined to the quantitatively reduced and qualitatively altered microvilli. This indicated that massive perturbation of the microvillar actin-based cytoskeleton does not abolish the specific localization of prominin in plasma membrane protrusions (see Supplementary information). Our conclusion that the retention of prominin in microvilli is not due to a direct interaction with the actin cytoskeleton is consistent with the previous observation[9] that deletion of the entire C-terminal tail, the most likely cytoplasmic domain of prominin to mediate such an interaction, does not perturb its microvillus-specific localization. Rather, prominin's dependence on cholesterol for its retention in microvilli suggests a specific protein–lipid interaction in the plane of the membrane as the primary cause of this retention.

Two types of Lubrol rafts containing prominin could be distinguished (see for example, Fig. 5b, Pro + Sap). One type, referred to as 'small' type, was sedimented by centrifugation for 1 h at 100,000*g* but not 10 min at 17,000*g* (Fig. 4a) and floated from fraction 8 to fractions 7 and 6 but not the low-density fractions 3–5 of the sucrose gradient (Fig. 4b). The other type, referred to as 'large' type, was already sedimented by centrifugation for 10 min at 17,000*g* (Fig. 1a) and floated to the low-density fractions 3–5 (Fig. 3b). Our pulse-chase analyses (Fig. 6a–c) indicate that the small type is assembled within the *trans*-Golgi/TGN and that its coalescence into the large type occurs concomitantly with the formation of the TGN-derived transport vesicle delivering prominin to the apical surface (Fig. 9). At the cell surface, cholesterol clustering increases (Fig. 5a, b), and cholesterol depletion decreases (Fig. 4), the ratio between large and small type (Fig. 9). This suggests that the coalescence of the small into the large type upon exit from the TGN, and perhaps the formation of apically destined TGN-derived transport vesicles as such, is a cholesterol-dependent process. This is consistent with the slowed cell-surface appearance of haemagglutinin and its mis-sorting to the basolateral side in MDCK cells[29] and the block of secretory vesicle formation from the TGN in AtT-20 cells (C. Thiele, Y. Wang and W.B.H, unpublished observations), which are observed upon cholesterol depletion. Extrapolating from the solubility of half of the cell-surface prominin in Lubrol WX upon cholesterol depletion using 50 mM mβCD in the cold, we conclude that the assembly of the small type of prominin-containing Lubrol raft in the TGN also involves cholesterol.

Assembly of the prominin-containing Lubrol raft in the TGN leaves us with two main possibilities of TGN-to-apical plasma membrane transport in polarized epithelial cells. First, there is only one type of apical transport vesicle, and both the 'classical' PLAP-containing Triton raft (which is also assembled in the TGN[29]) and the novel prominin-containing Lubrol raft described here are delivered in this vesicle to the apical plasma membrane (Fig. 9b). This implies that upon their arrival at the apical cell surface, these two types of raft physically segregate into the planar and microvillar subdomains, respectively. Second, there are two types of apical transport vesicles, as recently proposed[43], the 'classical' one that delivers the PLAP-containing Triton raft to the planar subdomain, and a new one that delivers the prominin-containing Lubrol raft to the microvillar subdomain (Fig. 9a). This implies the physical segregation of these two types of rafts upon exit from the TGN. Whichever of these two scenarios is the case, our results raise the intriguing possibility that the previously reported dual targeting of prominin, that is its sorting into an apical transport vesicle and its specific retention in microvilli within the apical membrane[9], has a common molecular basis, that is its incorporation in the TGN into a microvillus-specific raft. □

Methods

For more detailed methods see Supplementary Information (see also refs 44–47).

Methyl-β-cyclodextrin treatment.

For biochemical analyses, pellets (≈7 µl or ≈50 µl) of prominin- or PLAP-transfected MDCK cells were resuspended in either 70 µl (7-µl pellet) or 200 µl (50-µl pellet) of ice-cold buffer A (150 mM NaCl, 2 mM EGTA, 50 mM Tris-HCl pH 7.5, 10 µg ml^{-1} aprotinin, 2 µg ml^{-1} leupeptin and 1 mM PMSF) containing the indicated concentration (0–50 mM) of methyl-β-cyclodextrin (mβCD, Fluka; substitution rate 1.7–1.9) and incubated for 30 min at 4 °C.

For immunofluorescence analyses, prominin- and/or PLAP-transfected MDCK cells grown on glass coverslips were incubated for 30 min at 4 °C with 100 µl per coverslip of Ca/Mg-PBS-BSA lacking or containing 50 mM mβCD. To reverse the effect of cholesterol depletion due to the mβCD treatment, mβCD-treated MDCK cells were incubated for 1 h at 37 °C in serum-free Eagles minimal essential medium (E-MEM) supplemented with 10% delipidated FCS and containing 2.5 mg ml^{-1} of a mβCD-cholesterol complex[27].

Detergent lysis and differential centrifugation.

Pellets (7-µl) of prominin- or PLAP-transfected MDCK cells were lysed at ≈1.5 mg protein ml^{-1} for 30 min on ice in 70 µl of ice-cold buffer A containing one of the following detergents (lysis buffer): Lubrol WX (Lubrol 17A17) (Serva), Triton X-100 (Merck), Lubrol PX (Sigma), Brij series (Sigma), Triton X-102 (Sigma), Triton X-114 (Boehringer Mannheim), Tween 20 (Sigma), octylglucoside (Boehringer Mannheim) and CHAPS (AppliChem). Unless indicated otherwise, all detergents were used at a concentration of 0.5%, except for CHAPS and octylglucoside which were used at 20 mM and 60 mM, respectively. In some experiments, the lysis buffer containing Lubrol WX contained 1 M rather than 150 mM sodium chloride, or the solubilization was performed at 37 °C instead of 4 °C. Cell lysates were centrifuged at 4 °C either for 10 min at 17,000*g* or for 1 h at 100,000*g*. The entire supernatant and pellet was analysed by SDS–PAGE followed by either immunoblotting (see below) or Coomassie blue staining.

Detergent lysis and sucrose flotation gradients.

In the standard condition, pellets (50-µl) of prominin- or PLAP-transfected MDCK cells were lysed at ≈3.5 mg protein ml^{-1} for 30 min on ice in 200 µl ice-cold buffer A containing either 0.5% Lubrol WX or Triton X-100. The resulting detergent lysate (250 µl) was brought to 1.2 M sucrose using 2.4 M sucrose in buffer A, placed at the bottom of a SW60 tube and overlaid with 1 ml of 0.9 M, 0.5 ml of 0.8 M, 1 ml of 0.7 M and 1 ml of 0.1 M sucrose in buffer A. In some experiments, 0.1% Lubrol WX was included in the sucrose gradient, and/or cells were lysed at ~ 1mg protein per ml. Samples were centrifuged at 4 °C for 14 h at 335,000*g*. After centrifugation, 500-µl fractions were collected from the top to the bottom of the gradient, the pellet was resuspended in 500 µl buffer A containing 1% Triton X-100, and 450-µl aliquots of each fraction were analysed by SDS–PAGE followed by immunoblotting.

For Fig. 3e, a 70-µl aliquot of fraction 7 of a flotation gradient prepared after lysis in Lubrol WX was diluted to 1.3 ml with buffer A and centrifuged for 1 h at 100,000*g*, all at 4 °C. The entire supernatant and pellet, as well as another aliquot of fraction 7, were analysed by SDS–PAGE followed by immunoblotting for prominin.

Immunofluorescence.

For cell-surface immunofluorescence, single and double labelling cell-surface immunofluorescence of transfected MDCK cells was performed as described[9], except that for double labelling cells were incubated at 4 °C first with either the rat monoclonal antibody 13A4 against prominin (10 μg ml^{-1}) or mouse monoclonal anti-PLAP (1:50) for 30 min, and then with WGA coupled to TRITC (1:300, Dianova) for 15 min.

For immunofluorescence of fixed cells, MDCK cells transfected with PLAP plus prominin, were fixed for 5 min on glass coverslips with 3.7% paraformaldehyde in PBS at 6–8 °C, followed by a 5 min fixation in methanol at –20 °C (ref. 46), and subjected to double immunofluorescence[9].

For immunofluorescence after detergent extraction, prominin-transfected MDCK cells were dipped four times for 5 s at room temperature in a large excess of lysis buffer containing either 0.5% Lubrol WX or 0.5% Triton X-100 and lacking protease inhibitors[47], fixed with 3% paraformaldehyde in PBS and subjected to immunofluorescence.

RECEIVED 2 MAY 2000; REVISED 14 JUNE 2000; ACCEPTED 29 JUNE 2000;
PUBLISHED 15 AUGUST 2000.

1. Rodriguez-Boulan, E. & Nelson, J. Morphogenesis of the polarized epithelial cell phenotype. *Science* **245**, 718–725 (1989).
2. Simons, K. *et al.* Biogenesis of cell-surface polarity in epithelial cells and neurons. *Cold Spring Harbor Symp. Quant. Biol.* **57**, 611–619 (1992).
3. Kerjaschki, D., Noronha-Blob, L., Sacktor, B. & Farquhar, M.G. Microdomains of distinctive glycoprotein composition in the kidney proximal tubule brush border. *J. Cell Biol.* **98**, 1505–1513 (1984).
4. Simons, K. & Ikonen, E. Functional rafts in cell membranes. *Nature* **387**, 569–572 (1997).
5. Harder, T. & Simons, K. Caveolae, DIGs, and the dynamics of sphingolipid-cholesterol microdomains. *Curr. Opin. Cell Biol.* **9**, 534–542 (1997).
6. Brown, D. A. & London, E. Structure and function of sphingolipid- and cholesterol-rich membrane rafts. *J. Biol. Chem.* **275**, 17221–17224 (2000).
7. Bretscher, A., Reczek, D. & Berryman, M. Ezrin: a protein requiring conformational activation to link microfilaments to the plasma membrane in the assembly of cell surface structures. *J. Cell Sci.* **110**, 3011–3018 (1997).
8. Weigmann, A., Corbeil, D., Hellwig, A. & Huttner, W. B. Prominin, a novel microvilli-specific polytopic membrane protein of the apical surface of epithelial cells, is targeted to plasmalemmal protrusions of non-epithelial cells. *Proc. Natl Acad. Sci. USA* **94**, 12425–12430 (1997).
9. Corbeil, D., Röper, K., Hannah, M. J., Hellwig, A. & Huttner, W. B. Selective localization of the polytopic membrane protein prominin in microvilli of epithelial cells - a combination of apical sorting and retention in plasma membrane protrusions. *J. Cell Sci.* **112**, 1023–1033 (1999).
10. Maw, M. A. *et al.* A frameshift mutation in prominin (mouse)-like 1 causes human retinal degeneration. *Hum. Mol. Genet.* **9**, 27–34 (2000).
11. Corbeil, D. *et al.* The human AC133 hematopoietic stem cell antigen is also expressed in epithelial cells and targeted to plasma membrane protrusions. *J. Biol. Chem.* **275**, 5512–5520 (2000).
12. Fiedler, K., Kobayashi, T., Kurzchalia, T. V. & Simons, K. Glycosphingolipid-enriched, detergent-insoluble complexes in protein sorting in epithelial cells. *Biochemistry* **32**, 6365–6373 (1993).
13. Melkonian, K. A., Chu, T., Tortorella, L. B. & Brown, D. A. Characterization of proteins in detergent-resistant membrane complexes from Madin-Darby canine kidney epithelial cells. *Biochemistry* **34**, 16167–16170 (1995).
14. Umbreit, J. N. & Strominger, J. L. Relation of detergent HLB number to solubilization and stabilization of D-alanine carboxypeptidase from *Bacillus subtilis* membranes. *Proc. Natl Acad. Sci. USA* **70**, 2997–3001 (1973).
15. Miseta, A. *et al.* Effect of non-lytic concentrations of Brij series detergents on the metabolism-independent ion permeability properties of human erythrocytes. *Biophys. J.* **69**, 2563–2568 (1995).
16. Kunimoto, M., Shibata, K. & Miura, T. Comparison of the cytoskeleton fractions of rat red blood cells prepared with non-ionic detergents. *J. Biochem. (Tokyo)* **105**, 190–195 (1989).
17. Fey, E. G., Wan, K. M. & Penman, S. Epithelial cytoskeletal framework and nuclear matrix-intermediate filament scaffold: three-dimensional organization and protein composition. *J. Cell Biol.* **98**, 1973–1984 (1984).
18. Ojakian, G. K. & Schwimmer, R. The polarized distribution of an apical cell surface glycoprotein is maintained by interactions with the cytoskeleton of Madin-Darby canine kidney cells. *J. Cell Biol.* **107**, 2377–2387 (1988).
19. Brown, D. A. & Rose, J. K. Sorting of GPI-anchored proteins to glycolipid-enriched membrane subdomains during transport to the apical cell surface. *Cell* **68**, 533–544 (1992).
20. Schroeder, R., London, E. & Brown, D. Interactions between saturated acyl chains confer detergent resistance on lipids and glycosylphosphatidylinositol (GPI)-anchored proteins: GPI-anchored proteins in liposomes and cells show similar behavior. *Proc. Natl Acad. Sci. USA* **91**, 12130–12140 (1994).
21. Dupree, P., Parton, R. G., Raposo, G., Kurzchalia, T. V. & Simons, K. Caveolae and sorting in the trans-Golgi network of epithelial cells. *EMBO J.* **12**, 1597–1605 (1993).
22. Sargiacomo, M., Sudol, M., Tang, Z. & Lisanti, M. P. Signal transducing molecules and glycosyl-phosphatidylinositol-linked proteins form a caveolin-rich insoluble complex in MDCK cells. *J. Cell Biol.* **122**, 789–807 (1993).
23. Scheiffele, P., Roth, M. G. & Simons, K. Interaction of influenza virus haemagglutinin with sphingolipid-cholesterol membrane domains via its transmembrane domain. *EMBO J.* **16**, 5501–5508 (1997).
24. Klein, U., Gimpl, G. & Fahrenholz, F. Alteration of the myometrial plasma membrane cholesterol content with beta cyclodextrin modulates the binding affinity of the oxytocin receptor. *Biochemistry* **34**, 13784–13793 (1995).
25. Cerneus, D. P., Ueffing, E., Posthuma, G., Strous, G. J. & van der Ende, A. Detergent insolubility of alkaline phosphatase during biosynthetic transport and endocytosis. Role of cholesterol. *J. Biol. Chem.* **268**, 3150–3155 (1993).
26. Harder, T., Scheiffele, P., Verkade, P. & Simons, K. Lipid domain structure of the plasma membrane revealed by patching of membrane components. *J. Cell Biol.* **141**, 929–942 (1998).
27. Thiele, C., Hannah, M. J., Fahrenholz, F. & Huttner, W. B. Cholesterol binds to synaptophysin and is required for biogenesis of synaptic vesicles. *Nature Cell Biol.* **2**, 42–49 (2000).
28. Bretscher, M. S. & Munro, S. Cholesterol and the Golgi apparatus. *Science* **261**, 1280–1281 (1993).
29. Keller, P. & Simons, K. Cholesterol is required for surface transport of influenza virus hemagglutinin. *J. Cell Biol.* **140**, 1357–1367 (1998).
30. Baeuerle, P. A. & Huttner, W. B. Tyrosine sulfation is a trans-Golgi-specific protein modification. *J. Cell Biol.* **105**, 2655–2664 (1987).
31. Huttner, W. B. *et al.* Biogenesis of neurosecretory vesicles. *Cold Spring Harbor Symp. Quant. Biol.* **60**, 315–327 (1995).
32. Tooze, S. A. & Huttner, W. B. Cell-free protein sorting to the regulated and constitutive secretory pathways. *Cell* **60**, 837–847 (1990).
33. Francis, S.A. *et al.* Rapid reduction of MDCK cell cholesterol by methyl-beta-cyclodextrin alters steady state transepithelial electrical resistance. *Eur. J. Cell Biol.* **78**, 473–484 (1999).
34. Brown, D. A., Crise, B. & Rose, J. K. Mechanism of membrane anchoring affects polarized expression of two proteins in MDCK cells. *Science* **245**, 1499–1501 (1989).
35. Danielsen, M. E. & van Deurs, B. A transferrin-like GPI-linked iron-binding protein in detergent-insoluble noncaveolar microdomains at the apical surface of fetal intestinal epithelial cells. *J. Cell Biol.* **131**, 939–950 (1995).
36. Verkade, P., Harder, T., Lafont, F. & Simons, K. Induction of caveolae in the apical plasma membrane of Madin-Darby canine kidney cells. *J. Cell Biol.* **148**, 727–739 (2000).
37. Montixi, C. *et al.* Engagement of T cell receptor triggers its recruitment to low-density detergent-insoluble membrane domains. *EMBO J.* **17**, 5334–5348 (1998).
38. Ilangumaran, S. & Hoessli, D. C. Effects of cholesterol depletion by cyclodextrin on the sphingolipid microdomains of the plasma membrane. *Biochem. J.* **335**, 433–440 (1998).
39. Madore, N. *et al.* Functionally different GPI proteins are organized in different domains on the neuronal surface. *EMBO J.* **18**, 6917–6926 (1999).
40. Breckenridge, W. C., Morgan, I. G., Zanetta, J. P. & Vincendon, G. Adult rat brain synaptic vesicles. II. Lipid composition. *Biochim. Biophys. Acta* **320**, 681–686 (1973).
41. Breckenridge, W. C., Gombos, G. & Morgan, I. G. The lipid composition of adult rat brain synaptosomal plasma membranes. *Biochim. Biophys. Acta* **266**, 695–707 (1972).
42. Costa de Beauregard, M-A., Pringault, E., Robine, S. & Louvard, D. Suppression of villin expression by antisense RNA impairs brush border assembly in polarized epithelial intestinal cells. *EMBO J.* **14**, 409–421 (1995).
43. Lipardi, C., Nitsch, L. & Zurzolo, C. Detergent-insoluble GPI-anchored proteins are apically sorted in fischer rat thyroid cells, but interference with cholesterol or sphingolipids differentially affects detergent insolubility and apical sorting. *Mol. Biol. Cell* **11**, 531–542 (2000).
44. Gorman, C., Howard, B. & Reeves, R. Expression of recombinant plasmids in mammalian cells is enhanced by sodium butyrate. *Nucleic Acids Res.* **11**, 7631–7648 (1983).
45. Bligh, E. G. & Dyer, W. J. A rapid method for total lipid extraction and purification. *Can. J. Biochem. Physiol.* **37**, 911–917 (1959).
46. Osborn, M., Johnsson, N., Wehland, J. & Weber, K. The submembraneous location of p11 and its interaction with the p36 substrate of pp60 src kinase in situ. *Exp. Cell Res.* **175**, 81–96 (1988).
47. Algrain, M., Turunen, O., Vaheri, A., Louvard, D. & Arpin, M. Ezrin contains cytoskeleton and membrane binding domains accounting for its proposed role as a membrane-cytoskeletal linker. *J. Cell Biol.* **120**, 129–139 (1993).
48. *Surfactants, Microbiocides and Dispersants: Handbook of Physical Properties* (Rohm and Haas Co., PA, 1986).
49. Aldrich Catalogue (1999–2000).
50. Grant, D. A. & Hjerten, S. Some observations on the choice of detergent for solubilization of the human erythrocyte membrane. *Biochem. J.* **164**, 465–468 (1977).
51. Van Ede, J., Nijmeijer, J. R., Welling-Wester, S., Orvell, C. & Welling, G. W. Comparison of non-ionic detergents for extraction and ion-exchange high-performance liquid chromatography of Sendai virus integral membrane proteins. *J. Chromatogr.* **476**, 319–327 (1989).

ACKNOWLEDGEMENTS

We thank D. Brown for the PLAP-transfected MDCK cells, D. Louvard for the villin-antisense Caco2 cells, D. Buck for the antibody against human prominin (AC133 antigen), C. Thiele for [^{3}H]photocholesterol, 10-azistearic acid, cholesterol–mβCD complex and delipidated sera, A. Hellwig for electron microscopy, and M.J. Hannah for help with confocal microscopy. K.R. was the recipient of a fellowship from the Studienstiftung des Deutschen Volkes. W.B.H. was supported by grants from the DFG (SFB 352, C1), the EC (ERB-FMRX-CT96-0023 and ERBBIO4CT960058), the German-Israeli Foundation for Scientific Research and Development, and the Fonds der Chemischen Industrie.

Correspondence and requests for materials should be addressed to W.B.H.

Supplementary Information is available on *Nature Cell Biology*'s World-Wide Web site (http://cellbio.nature.com) or as paper copy from the London editorial office of *Nature Cell Biology.*